Remote Sensing of Environment 133 (2013) 116–127

Contents lists available at SciVerse ScienceDirect

Remote Sensing of Environment

journal homepage: www.elsevier.com/locate/rse

Suitability of OMI aerosol index to reflect mineral dust surface conditions: Preliminary application for studying the link with meningitis epidemics in the Sahel

A. Deroubaix [a,b,*], N. Martiny [a], I. Chiapello [c], B. Marticorena [d]

[a] Biogéosciences/CRC, UMR 6282 CNRS/Université de Bourgogne, France
[b] LOCEAN, UMR 7617 CNRS/IRD/UPMC, IPLS, Paris, France
[c] LOA, UMR 8518 CNRS/Université Lille 1, France
[d] LISA, UMR 7583 CNRS, UPEC-UPD, IPSL, France

ARTICLE INFO

Article history:
Received 2 March 2012
Received in revised form 6 February 2013
Accepted 7 February 2013
Available online xxxx

Keywords:
Mineral dust
Aerosol index
AOT
Surface concentration
Meningitis

ABSTRACT

The aim of this study is to analyze the suitability of remotely-sensed aerosol retrievals to progress in the understanding of the influence of desert dust on health, and particularly on meningitis epidemics. In the Sahel, meningitis epidemics are a serious public health issue. Social factors are of prime importance in the dynamics of the epidemics, however climate and environmental factors are also suspected to play an important role.

This study focuses on three Sahelian countries (Burkina Faso, Mali and Niger) which are among the most concerned in the "meningitis belt" and affected by strong dust events every year. It investigates the capability of the aerosol index (AI) derived from OMI (ozone monitoring instrument) to represent the aerosol optical thickness (AOT) and the aerosol surface concentration (particulate matter <10 μm; PM_{10}) at different time-steps. The comparison of the OMI-AI with ground-based measurements of AOT shows a good agreement at a daily time-step ($R \approx 0.7$). The correlation between OMI-AI and PM_{10} measurements is lower ($R \approx 0.3$) but it increases at a weekly time-step ($R \approx 0.5$). The difference in the level of correlation between the AOT and the PM_{10} is partly related to changes in the altitude of the dust layers, especially from April to June, the period of transition from the dry to the wet season. A temporal shift is observed in the occurrence of the maximum of PM_{10} concentration (March), of AOT (April) and of OMI-AI (June). Nevertheless, during the core of the dry season (January to March) when dust is transported at low altitude, the OMI-AI is able to correctly detect the dust events and to reproduce the dust variability at the regional scale.

For dust impact studies on health, only the surface level is relevant. Thus, we conclude that the OMI-AI is suitable especially at a weekly time-step from January to March. In particular for meningitis impact studies, it appears as suitable from the onset to the maximum of the epidemics. A preliminary investigation of the link between the OMI-AI and the WHO weekly national epidemiological reports reveals a 1-week time-lag between the occurrence of dust and meningitis during the increasing phase of the disease.

1. Introduction

The largest sources of mineral aerosols of the world have been proved to be located in the Sahara (Goudie & Middleton, 2001). Both models and observations show that Saharan dust yield over 40% of the global aerosol production from natural sources (Laurent et al., 2008; Ramanathan et al., 2001; Zender & Kwon, 2005). Mineral dust impacts the climate, through direct and indirect radiative forcing (Sokolik et al., 2001). The impact on human health has been demonstrated in several places far away from the Sahara (De Longueville et al., 2009), for instance with the daily mortality in Spain (Perez et al., 2008) or with asthma attacks in the Caribbean islands (Gyan et al., 2005; Prospero et al., 2008). Although the European or American air quality standards for particulate matter smaller than 10 μm (PM_{10}) concentration are currently widely exceeded in the Sahel (Marticorena et al., 2010; De Longueville et al. (2010) deplores the lack of mineral dust impact studies on health in this area due to the lack of air quality monitoring stations.

In West Africa, the meningococcal meningitis (bacteria: *Neisseria meningitidis*, serogroups: A, C, W135 and X) outbreaks are a major public health problem and the serogroup A is responsible for 85% of the cases (Campagne et al., 1999). For instance 200,000 cases have been recorded (Greenwood, 1999) in 1996 throughout the "Meningitis Belt" defined by Lapeyssonnie in 1963. About 300 million people live in this area, which extends from Senegal to Ethiopia on a 10–15° North latitudinal band. According to the World Health Organization (WHO), 10 to 20% of the cases are lethal and 10 to 20% of the survivors present neurological sequels. Social factors like number of people per house, exposure to smoke, immunity and population dynamics are critical to understand the spread of the bacteria. The major dust outbreaks occur

* Corresponding author at: UMR 6282 CNRS/Université de Bourgogne, Biogéosciences/Centre de Recherches de Climatologie, 6 Boulevard Gabriel, Bâtiment Sciences Gabriel, 21000 Dijon, France. Tel.: +33 3 80 39 38 21; fax: +33 3 80 39 57 41.
E-mail address: adrien.deroubaix@u-bourgogne.fr (A. Deroubaix).

0034-4257/$ – see front matter © 2013 Elsevier Inc. All rights reserved.
http://dx.doi.org/10.1016/j.rse.2013.02.009

during the winter dry season (December to April) dominated by warm and dry dust-laden winds coming from the North (Harmattan winds). Up to recently the influence of mineral dust on meningitis epidemics had been only suggested, with several possible mechanisms of interactions not fully understood (Thomson et al., 2006, 2009), as discussed in Section 3.3.

Recent studies achieved in the frame of the AMMA (African Monsoon Multidisciplinary Analyses) program strengthen the hypothesis of a significant impact of high dust load on meningitis epidemics in the Sahelian countries (Martiny & Chiapello, in press). Given the lack of ground-based dust measurements in this region, important progress would be made by using dust remote sensing products to investigate the role of the dust on meningitis epidemics. The use of long time series of aerosol products is required and quantitative products of aerosol optical thickness (AOT) are retrieved over continental surfaces from now on. AOT derived from MODIS (MODerate Imaging Spectro-radiometer) using the so-called "deep blue" algorithm (Hsu et al., 2004) has been calculated retrospectively for the period (1999–2010) but has not been deeply tested and validated over the North of Africa. AOT retrievals are also available from the multi-angle imaging spectroradiometer (MISR) and have been tested over desert sites (Martonchik et al., 2004). While several authors recognized the quality of the MISR AOT, their use for climatologic studies is limited by a poor spatial sampling (Christopher et al., 2008). The intercomparison of the most recent AOT products over land reveals large differences attributed to differences in the sensors and especially in the retrieval algorithms (Carboni et al., 2012).

Two semi-quantitative aerosol products, used for mineral dust climatology, are available for a longer period over the North of Africa. The infrared difference dust index (IDDI) is derived from the Meteosat radiances at the top of the atmosphere in the thermal infrared (10.5–12.5 μm) by Legrand et al. (1989). The IDDI is available at a 1° spatial resolution over Africa but only for the period 1984–1993 (Legrand et al., 2001). The AI (absorption aerosol index) product (Herman et al., 1997; Torres et al., 1998) is derived from radiances in the UV (at two wavelengths 354 nm and 388 nm). The AI algorithm was first applied to data from the TOMS (total ozone mapping spectrometer) sensors on Nimbus (1978–1993) and Earth-Probe (1996–2005) missions. Since 2004 the successor of TOMS, the OMI (ozone monitoring instrument) provides an AI product at a 0.25° spatial resolution. The perspective to link the TOMS-AI and the OMI-AI offers a chance to create the longest time-series relevant for the dust in desert areas. Indeed, the AI has been proved to be highly performing over continental surfaces like desert or semi-arid environments because the reflectivity of these surfaces in UV is low (Eck et al., 1987; Herman & Celarier, 1997). Like most of the satellite aerosol retrievals, the TOMS and OMI AI products have been validated by comparison to the NASA Aerosol Robotic Network (AERONET) sun photometer aerosol optical thickness (AOT) (Holben et al., 1998) at a global scale (Hsu et al., 1999; Torres et al., 2002, 2007). The AI has been widely used in the geophysical fields, for instance to characterize the dust sources over the Sahara (Engelstaedter et al., 2006; Prospero et al., 2002; Washington et al., 2003). Decadal trend studies of the dust transport over the North Atlantic have been achieved (Chiapello & Moulin, 2002; Chiapello et al., 2005) and the ability of TOMS-AI to detect the Saharan events has been demonstrated in comparison with PM_{10} measurements at four remote places (Chiapello et al., 1999). Despite the sensitivity of the AI to the aerosol plume height, the AI is able to represent the dust features at the ground level as detecting dust event over continent and ocean (Chiapello et al., 1999; Ginoux & Torres, 2003). Recently, the OMI-AI has been used to improve the AOT retrieval from MODIS (Satheesh et al., 2009) or MISR in the North of Africa (Christopher et al., 2008). The TOMS-AI has already been used for meningitis impact studies in West Africa (Molesworth et al., 2003; Thomson et al., 2006). Among a set of societal, climate and environment variables, these studies conclude that dust is one of the most important risk factors for meningitis. Nonetheless the authors recommend to examine the ability of satellite proxies to represent the dust concentrations at the ground level. The main motivation of this work is thus to evaluate the suitability of OMI-AI for health impact studies in West Africa and more specifically its capability to represent the surface concentration at the period of the meningitis epidemics in the Sahel.

This analysis focuses on Burkina Faso, Mali and Niger, which are among the most affected countries in the meningitis belt (Molesworth et al., 2002) and markedly affected by strong dust events every year (Morales, 1986; N'Tchayi et al., 1994). During the dry season from October to April, the Harmattan wind blows over the Sahel carrying mineral aerosols in the boundary layer (Léon et al., 2009). High aerosol concentrations at the surface are recorded every year during the core of the dry season (defined as January to March) due to transport at the continental scale (Marticorena et al., 2010). Our strategy is to examine, at different time-steps and periods of the year, coincident measurements of dust concentration recorded at the ground level which can be related to population exposure rates, ground based AOT data, and the OMI-AI retrievals. The OMI-AI, the AOT and the PM_{10} are three independent measurements that all document the atmospheric aerosol load. The OMI-AI is a semi-quantitative parameter which has been shown to depend on the AOT that quantifies the extinction of visible radiation proportional to the vertically integrated aerosol atmospheric content. The PM_{10} surface concentration is linked, to some extent, to the column concentration. But its representativity depends on the altitude and homogeneity of the dust layers. Two major questions are addressed in this study: (i) At which time-step are the OMI-AI, AOT and PM_{10} in the best agreement in typical Sahelian sites? (ii) During which period is the OMI-AI able to reproduce the variability of the dust surface concentration? Section 2 describes the data sets and the methodology. Section 3 presents the OMI-AI compared to the AOT data sets from AERONET (Section 3.1) and to PM_{10} measurements (Section 3.2), and ends by a preliminary analysis on meningitis epidemics at the national level (Section 3.3). The results are discussed and the conclusions are given in Section 4.

2. Data and methods

2.1. Aerosol index from the OMI satellite sensor

The OMI sensor is onboard the Aura spacecraft of the NASA Earth Observing System in the A-train. The equator crossing time of the "Afternoon train" is 13:45 (Levelt et al., 2006). Global daily level 3 (average covering the whole globe from 14 single orbits acquired each day) AI products are available since October 2004 at a spatial resolution of 13∗24 km at nadir. The AI product is the spectral contrast of the effective radiance with aerosol effects and calculated radiance in the UV based on the radiative transfer theory and given a pure molecular atmosphere (i.e., Rayleigh particles for which the diameter is largely inferior to the wavelength of the incident signal). The AI has first been defined for TOMS radiances at 340 and 380 nm by Torres et al. (1998) and modified for OMI using the radiances at 354 and 388 nm by Torres et al. (2007) following:

$$AI = -100 \ \log_{10}\left(I^{354}obs/I^{354}calc\right) \quad (1)$$

where $I^{354}obs$ is the effective radiance observed at the top of the atmosphere and $I^{354}calc$ is the radiance estimated from I^{388}. AI positive values are associated with absorbing aerosols in the UV, mainly from mineral and volcanic aerosols as well as biomass burning, and negative values are associated with non-absorbing aerosols like sea salt particles.

Fig. 1 presents the 2005–2008 averaged AI from OMI in Africa North of the equator. In the Sahara, the OMI-AI reaches as high as those values previously obtained with TOMS-AI for the same locations (Engelstaedter & Washington, 2007a; Goudie & Middleton, 2001; Prospero et al., 2002; Washington et al., 2003). The region of the Bodélé depression in Chad recognized as the most active dust source (Engelstaedter et al., 2006; Washington et al., 2006) experiences the highest values (≈3.5) whereas

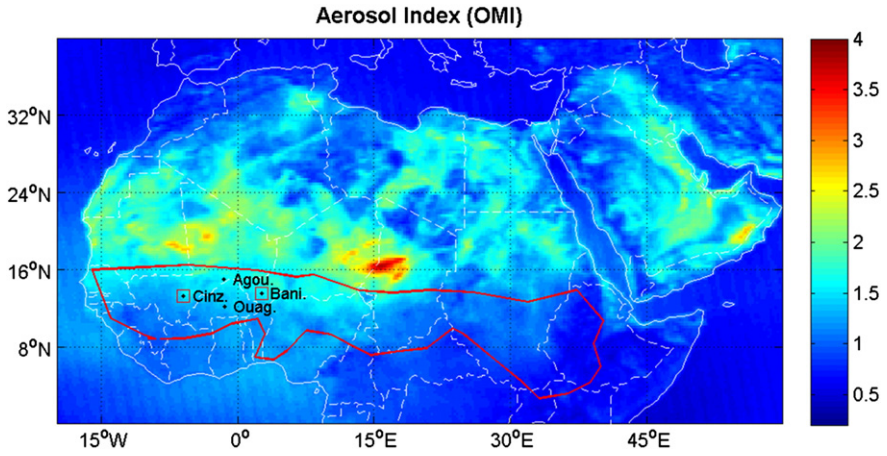

Fig. 1. West Africa long-term mean OMI-AI (at 0.25∗0.25°) averaged over 4 entire years (2005 to 2008). AERONET/PHOTONS Cinzana (Mali), Agoufou (Mali), Ouagadougou (Burkina Faso), Banizoumbou (Niger) used in this study are reported. Square indicates sites providing TEOM PM_{10} used in this study. The meningitis belt is indicated in red. (For interpretation of the references to color in this figure, the reader is referred to the web version of this article.)

more moderate values (≈2.5) are recorded for sources along the border between Mali and Mauritania or in South Algeria.

The OMI-AI values were extracted for the pixels corresponding to the four AERONET sites (locations indicated in Fig. 1, black dots) and the 8 surrounding pixels. A square of 3×3 OMI-AI pixels is thus averaged for each site, every day, for the period 2005–2008 (after 2009 the OMI sensor suffers from raw anomalies). Within those 9 pixels, the average AI is computed for AI higher than 0.2 to avoid cloud contamination (Torres et al., 2002).

2.2. Aerosol optical thickness

AERONET is an aerosol network constituted of autonomous sun photometers (Holben et al., 1998) deployed over more than 500 ground-based stations throughout the world. Within the AERONET/PHOTONS component in West Africa, four stations have been selected based on the temporal depth of their data sets and their common time-period with the OMI-AI (Fig. 1). There are two sites in Mali (Cinzana and Agoufou), one site in Burkina Faso (Ouagadougou) and one site in Niger (Banizoumbou). The period covered by the selected data sets is 2005–2009, except in Ouagadougou, for which the period is reduced to 2005–2007 (January). For the sun photometers of these sites, the irradiance (W/m^2) are measured in five spectral bands (440, 675, 870, 940, and 1020 nm) in order to retrieve the aerosol optical thickness (AOT) and the Angstrom exponent (α), at a 15-min time-step during the day. In this study, we consider the AOT at the 440 nm, which is the closest wavelength from UV (referred to as AOT_{440} in the following) and the $\alpha_{440/870}$ representative of an average aerosol spectral dependency according to the Angstrom law between 440 nm and 870 nm. The current study is based on level 2 AOT_{440} and $\alpha_{440/870}$, which are high-quality AERONET products corrected for clouds. Fig. 2 illustrates the daily mean AERONET L2 AOT_{440} and $\alpha_{440/870}$ data sets in Banizoumbou (Niger) in 2006. The AOT_{440} presents a clear seasonal cycle (Fig. 2a), with high daily values (reaching 4) in AOT_{440} from March to June, low values (below 1) from July to November, and intermediate values (1 to 2) from December to February. A dust outbreak is characterized by high AOT values associated with low Angstrom exponents (Pinker et al., 2001). The $\alpha_{440/870}$ ranges from −0.1 to 1.3 (Fig. 2b). On the 8th of March 2006, $\alpha_{440/870}$ reaches 0.2 when the yearly AOT_{440} maximum of 2006 is recorded. From February to June, it is lower than 0.5 (threshold on Fig. 2a and b), which clearly indicates the presence of coarse particles like the Saharan dust. On the contrary, $\alpha_{440/870}$ is generally greater than 0.5 from July to January, indicating the presence of finer particles (Haywood et al., 2008). In particular, in December and January, the AOT is impacted by the presence of carbonaceous aerosols emitted from biomass burning (Ogunjobi et al., 2008). A threshold of 0.5 on $\alpha_{440/870}$ (Fig. 2a) is efficient to distinguish situations where mineral dust is dominant (Smirnov et al., 2000). For Banizoumbou, Fig. 2b highlights that high AOT_{440} values (>1) are associated with dust particles, as they present a low spectral dependency (i.e., $\alpha_{440/870}<0.5$), whereas the AOT_{440} between 0 and 1 may be associated with a mixture of large dust and fine particles. Those behaviors are typical of the Sahelian stations (Holben et al., 2001) and are observed at the three other selected sites (not shown).

In our analysis, we compare the satellite retrievals (i.e., OMI-AI) to the coincident ground-based AOT_{440} measured by the sun photometers. The AOT_{440} is first extracted at the closest satellite overpass time ±1 h. The average of the AOT_{440} values is computed only if a minimum of two AOT_{440} measurements were available in 1 h (stability criteria). Then, in order to test if the OMI-AI is representative of the AOT_{440} measured during the day, the AOT_{440} was extracted at the satellite overpass time ±5 h. The average of the AOT_{440} values was computed only if a minimum of ten AOT_{440} measurements were available during these 5 h (stability criteria). For our comparisons, we use the $\alpha_{440/870}$ threshold of 0.5 to distinguish the mineral dust events from the cases influenced by other aerosol species.

2.3. PM_{10} concentration measurements

The atmospheric concentrations of particulate matter lower than 10 μm in diameter (PM_{10}) have been acquired since January 2006 in the frame of the AMMA program at three Sahelian stations (Marticorena et al., 2010). The stations (Fig. 1, red squares) are located along the main dust transport pathway towards the Atlantic Ocean (near 13°N), in Banizoumbou (Niger), Cinzana (Mali) and M'Bour (Senegal) composing the Sahelian Dust Transect (SDT). They are all equipped with AERONET/PHOTONS sun photometers. Note that the data from the site of M'Bour are not considered here because the aerosol concentrations are affected by oceanic influences and anthropogenic aerosol sources; furthermore meningitis outbreaks seldom affect Senegal.

The PM_{10} concentration is determined at a 5-min time-step by a tapered element oscillating microbalance (TEOM) instrument equipped with a PM_{10} inlet (Marticorena et al., 2010). Fig. 3 presents the PM_{10} cycle measured in Banizoumbou in 2006 at different time-steps: the monthly scale highlights the annual cycle, while weekly/daily scales are more suitable for the impact analysis. The PM_{10} seasonal cycle presents similarities with that of AOT_{440} (Fig. 2a). Low values (below 100 $\mu g/m^3$) are observed from July to November, and intermediate values (100 $\mu g/m^3$ to 1000 $\mu g/m^3$) from December to June. Extremely high PM_{10} concentrations are monitored in this region and three main

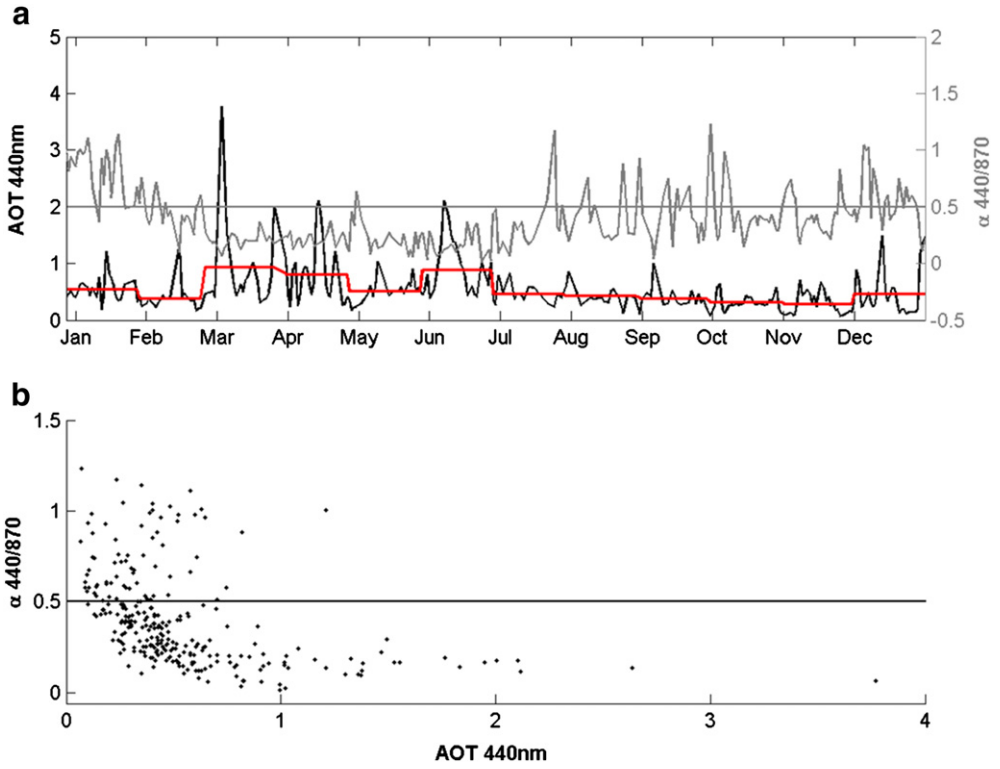

Fig. 2. a) Daily variation of AOT_{440} (black line) and $\alpha_{440/870}$ (gray line) retrieved from AERONET/PHOTONS sun photometers at Banizoumbou (Niger) in 2006. The red line is the monthly average of AOT_{440} and the gray line shows the threshold of the Angstrom exponent at 0.5; b) scatter plot of daily $\alpha_{440/870}$ versus daily AOT_{440} at Banizoumbou (Niger) in 2006. (For interpretation of the references to color in this figure, the reader is referred to the web version of this article.)

peaks are observed in Fig. 3: in December and in March during the core of the dry season due to regional dust transport; and in June at the beginning of the wet season due to local mesoscale convective system (Marticorena et al., 2010). The choice of the time-step is essential to focus on a specific process, for instance concentration reaches 3410 μg/m^3 for the daily average (in June), 1046 μg/m^3 for the weekly average (in March), 407 μg/m^3 for the monthly average (in March); but concentration reaches 4812 μg/m^3 at a 5-min time-step (in June; not shown in Fig. 3). To compare OMI-AI with PM_{10} data sets, we use the same temporal averages as for ground-based AOT_{440} except that a

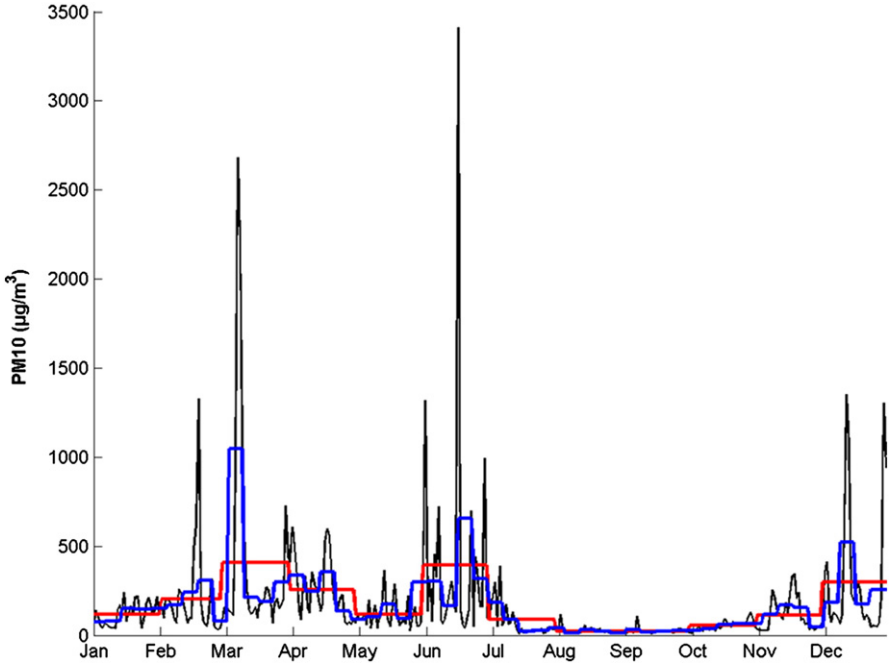

Fig. 3. PM_{10} concentrations measured by TEOM in μg/m^3 for different average steps (daily: black line/weekly: blue line/monthly: red line) during 2006 in Banizoumbou (Niger). (For interpretation of the references to color in this figure, the reader is referred to the web version of this article.)

supplementary 24-hour average is computed in order to investigate the importance of diurnal variations (no criterion on the number of available measurements per hour is applied).

2.4. Meningitis data set

The weekly surveillance of the meningococcal meningitis is made by the World Health Organization (WHO). A data set of the number of "suspected" cases recorded in the meningitis belt over three years (2005 to 2007) already used in Agier et al. (2013), has been used in this study. The national incidence (referred as "NI" in the following) is this number of cases divided by the population. Recently, this data set has been used to investigate the link between climate factors and meningitis outbreaks in Mali (Sultan et al., 2005), Burkina Faso, and Niger (Yaka et al., 2008).

2.5. Statistical methodology

This analysis only uses descriptive statistics; the scatter plot of the OMI-AI with ground-based data sets (AOT_{440} or PM_{10}) is characterized by a distribution ellipse. After the standardization of the two data sets: (X − meanX)/stdX and (Y − meanY)/stdY (std stands for standard deviation), the main axis is obtained by minimizing the orthogonal distance to the regression line. The orthogonal regression or major axis regression (i.e., the slope and intercept of this line) is calculated instead of the ordinary least square because it is more suitable for remotely sensed measurements (Cohen et al., 2003). This method involves the uncertainties of both variables, and it allows describing the scatter plot at each station as explained by Ayers (2001) in the context of PM_{10} measurement for air quality. The correlation coefficient reflects the noisiness of the linear relationship, defined as R = covXY/(stdX ∗ stdY), X and Y being respectively the OMI-AI and the AOT_{440} or the PM_{10} time-series. The significance threshold is obtained based on a Monte-Carlo test, it consists in 1000 random permutations of the data and 1000 random R computed: the significance threshold is the percentile 95 (i.e., the 950th highest value). This is more adequate than the classical Bravais–Pearson significance test regarding the autocorrelation of the time-series used in the current study (Mann et al., 1998).

3. Results

3.1. Analysis of the OMI-AI/AOT_{440} relationship

3.1.1. Influence of the Angstrom exponent

In the Sahel mineral dust can be mixed with other aerosols, in particular with carbonaceous aerosols from biomass burning in the beginning of the dry season (Haywood et al., 2008). Here a threshold of 0.5 for $\alpha_{440/870}$ (Section 2.2) is used to distinguish mineral dust cases from mixed aerosol situations. Fig. 4 presents the scatter plot between OMI-AI and AOT_{440} considering every common day of the period 2005–2008 in Cinzana, Agoufou and Banizoumbou and the period 2005–2006 in Ouagadougou. The number of "dusty" days is approximately the same for the different sites (between 800 and 900) except in Ouagadougou for which the studied period is restricted to 2005–2006 (about 200 points). The correlation coefficients between OMI-AI and AOT_{440} are always significant. They range from 0.6 in Cinzana to 0.7 in Agoufou, Banizoumbou and Ouagadougou. These results are in agreement with previous studies performed between the TOMS-AI and the AOT from AERONET (Hsu et al., 1999; Torres et al., 2002). It is interesting to note that the slopes of the linear regressions slightly vary from East to West, being greater in Cinzana (1.98) than in Banizoumbou (1.47), while Agoufou and Ouagadougou show intermediate values (1.89 and 1.77 respectively). Considering the cases corresponding to "all aerosols" (gray symbols and lines) with the influence of both dust and biomass burning particles adds about 20% of data at each site. These cases generally correspond to low AOT_{440} and OMI-AI values, so their weight in the linear regression may be weak.

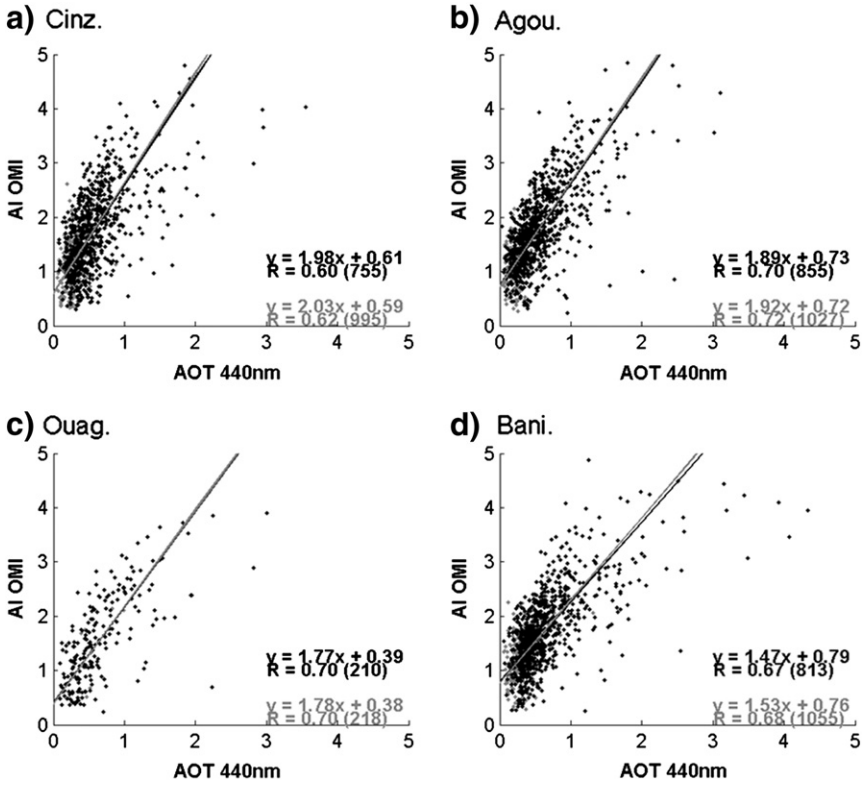

Fig. 4. Scatter plot between OMI-AI and AOT_{440} extracted at the satellite overpass time ±1 h for every common day of the period 2005–2009 in a) Cinzana (Mali). b) Agoufou (Mali). c) Ouagadougou (Burkina Faso). d) Banizoumbou (Niger). The linear regression standing for dust aerosols (all aerosols) is indicated in black (gray).

The correlation coefficients between OMI-AI and AOT_{440} for "all aerosols" cases are slightly higher than those obtained for the "dust" situations, and all are significant (0.62 in Cinzana, 0.70 in Ouagadougou, 0.68 in Banizoumbou, and 0.72 in Agoufou). For the four sites, the slopes are very close to those previously obtained for the "dust" cases. The influence of the aerosol type, as inferred from the Angstrom exponent, can be considered as limited. This seems to be due to the higher frequency of "dust" cases compared to mixed aerosol cases (the latter representing about 20%), and the highest aerosol loads are related to the "dust" cases. This result evidences that the influence of other aerosol types than dust on OMI-AI can be neglected in the Sahel.

3.1.2. Seasonality

Correlation coefficients between OMI-AI and AOT_{440} are computed considering every common day of the whole year, and every common day during the core of the dry season (Table 1). For the two periods at all four sites, the correlation coefficients are significant and comparable (between 0.62 and 0.73). Table 2 presents the slopes and intercepts of the linear regressions; for the whole year (the core of the dry season) the slopes vary from the East: 1.53 (1.22) in Banizoumbou to the West: 2.03 (1.63) in Cinzana. For a given OMI-AI, the AOT_{440} is higher during the core of the dry season than during the whole year because AI from OMI better captures the dust events moving at high altitude than the dust events moving close to the surface (Mahowald & Dufresne, 2004; De Graaf et al., 2005). During the dry season, the dust events which flow at relatively low altitude (Cavalieri et al., 2010) are retrieved by OMI with a weaker AI signal and the slopes of the major axis regression are all lower. Overall, these results confirm that the OMI-AI is significantly related to the AOT_{440}, whatever the period of the year.

3.1.3. OMI-AI representativity of daily integrated AOT_{440}

As a spatial integration, we use 8 OMI pixels surrounding the pixel of every sun photometer station (Section 2.1). This average of OMI-AI is then compared to the temporally AOT_{440} averaged: (i) at ± 1 h around the satellite overpass time, (ii) at ± 5 h around the satellite overpass time. The correlation coefficients (Table 3) between the OMI-AI and the AOT_{440} are almost the same (about ≈ 0.7) when considering the daily average (± 5 h) compared to ± 1 h overpass and the slopes remain stable (not shown). The lowest correlation (0.62) is obtained at the overpass time for Cinzana; it increases to 0.65 at the daily average. For each site, the major axis regression parameters (slopes and intercepts) are similar at a 5% error confidence interval from the overpass time to the daily average. Thus, at each site and for each period, the correlation coefficients are high enough to consider that the OMI-AI is representative of the daily mean AOT_{440}.

3.1.4. AOT_{440} as a proxy of PM_{10}

AOT have already been used as an estimate of the PM_{10} at ground level (Pelletier et al., 2007; Péré et al., 2009; Yahi et al., 2011) in several places of the world, but mainly in urban environments. Some of these studies (Pelletier et al., 2007; Yahi et al., 2011) used hierarchical classification and clustering to improve the relationship between the AOT and the surface concentration by distinguishing different meteorological patterns.

Table 1
Annual and seasonal correlation coefficients between OMI-AI and AOT_{440} extracted at the satellite overpass time ± 1 h for the whole year and considering only the core of the dry season (i.e., from January to March).

	Whole year		Core dry season	
	R	*N*	*R*	*N*
Cinzana	0.62	995	0.65	584
Agoufou	0.72	1027	0.69	538
Ouagadougou	0.70	218	0.71	125
Banizoumbou	0.68	1055	0.73	603
All sites	0.66	3295	0.69	1850

Table 2
Annual and dry season slope and intercept of the linear regression between OMI-AI and AOT_{440} extracted at the satellite overpass time ± 1 h for the whole year and considering only the core of the dry season (i.e., from January to March).

	Whole year		Core dry season	
	Slope	Intercept	Slope	Intercept
Cinzana	2.03	0.59	1.63	0.82
Agoufou	1.92	0.72	1.63	0.87
Ouagadougou	1.78	0.38	1.60	0.53
Banizoumbou	1.53	0.76	1.22	0.94
All sites	1.78	0.69	1.44	0.87

Such studies have not yet been achieved in the Sahel, partly due to the lack of surface aerosol concentration measurements. In this region, the relationship is expected to vary with the time of day, and also between the dry and wet seasons because the altitude of the dust layer changes. Table 4 presents the correlation coefficients between the AOT_{440} and PM_{10} concentrations temporally averaged over the entire year at different time-steps: (i) at ± 1 h around the satellite overpass time ("overpass"), (ii) at ± 5 h around the satellite overpass time ("day"), (iii) at ± 12 h around the satellite overpass time ("24 h"), and (iv) over a week (a weekly average of the daily values). When increasing the integration time from 1 h to 1 week, the correlation coefficients remain stable ($R \approx 0.60$) in Cinzana. In particular, no difference is observed between the ± 5 h ("day") and the 24 h (day + night) concentration averages. In Banizoumbou, the correlation coefficients decrease from the 5-hour average (i.e., daytime only) to the 24-hour average (i.e., daytime and nighttime) from 0.68 to 0.44. This suggests that the influence of the diurnal dust cycle is stronger in Banizoumbou than in Cinzana. By focusing on the core of the dry season, an improvement of the correlation coefficient is observed for every temporal average, especially for the weekly average in Banizoumbou from 0.64 to 0.82 and in Cinzana from 0.79 to 0.93. Finally, the use of the daily or weekly averages gives comparable correlations to those obtained with the hourly averages at the OMI overpass time in Cinzana and Banizoumbou. These results suggest that in the Sahel, the AOT can be used as an estimate of the PM_{10} at the ground level, especially at a weekly time-step during the core of the dry season.

3.2. Suitability of the OMI-AI for the investigation of dust impact on meningitis

3.2.1. Analysis of the OMI-AI/PM_{10} relationship

The aerosol concentrations (PM_{10}) have been temporally averaged and compared with the daily OMI-AI at the stations of Banizoumbou (Niger) and Cinzana (Mali) since 2006 (Table 5) for the whole year. The correlation coefficients between the OMI-AI and PM_{10} at the time of the satellite overpass (or at a daily time-step) are weaker compared to those obtained with the AOT_{440} (Table 5 versus Table 3): 0.34 versus 0.62 (overpass time) and 0.36 versus 0.65 (daily time-step) in Cinzana; 0.40 versus 0.68 (overpass time) and 0.37 versus 0.69 (daily time-step) in Banizoumbou. It shows that the OMI-AI is a better indicator of the vertically integrated dust amount than of the surface concentrations. This result was somehow expected, as both the OMI-AI and AOT_{440}

Table 3
Correlation coefficients between OMI-AI and AOT_{440} extracted at the satellite overpass time ± 1 h (overpass column) and extracted at the satellite overpass time ± 5 h (column "day") for the whole year.

	Overpass		Day	
	R	*N*	*R*	*N*
Cinzana	0.62	995	0.65	995
Agoufou	0.72	1027	0.73	1027
Ouagadougou	0.70	218	0.70	218
Banizoumbou	0.68	1055	0.69	1055
All sites	0.66	3295	0.68	3295

Table 4
Correlation coefficients between AOT_{440} and PM_{10}concentrations temporally averaged at ±1 h around the satellite overpass time (column "overpass"), at ±5 h around the satellite overpass time (column "day"), at ±12 h around the satellite overpass time (column "24 h"), at a weekly time-step for the whole year.

	Overpass		Day		24 h		Weekly	
	R	*N*	*R*	*N*	*R*	*N*	*R*	*N*
Cinzana	0.60	799	0.58	813	0.59	813	0.64	151
Banizoumbou	0.81	771	0.68	776	0.44	776	0.79	144
All sites	0.73	1570	0.64	1589	0.46	1589	0.73	295

parameters are optical parameters integrated over the atmospheric column, contrary to PM_{10} which results from surface measurements. At a 24-hour time-step, the OMI-AI/PM_{10} correlation is weaker in Banizoumbou (0.27) than in Cinzana (0.36), which may be explained by a stronger diurnal cycle of the concentrations in Banizoumbou than in Cinzana, as previously shown by the PM_{10}/AOT_{440} relationship (Section 3.1.4). In order to progress in our evaluation of the suitability of the OMI-AI for health impact studies, and specifically meningitis epidemics, we now examine a longer time-step.

3.2.2. OMI-AI at the 1-week epidemiological time-step

As the meningitis epidemiological reports are available at a weekly time-step, we compared the OMI-AI to the AOT_{440} and the PM_{10} at this time-step. An improvement of these relationships is expected at a weekly time-step because it reduces the range of variation; i.e., the standard deviation of both OMI-AI and AOT_{440} (or PM_{10}) is lower than at a daily time-step. The goal of this section is to quantify this improvement. Fig. 5 presents the scatter plots of the OMI-AI versus the AOT_{440} and versus the PM_{10} in Cinzana (Fig. 5a and b), and Banizoumbou (Fig. 5c and d). From the daily to the weekly time-step, the correlation coefficients increase by 10% for the OMI-AI/AOT_{440} and 30% for the OMI-AI/PM_{10} relationship. In Cinzana, the correlation coefficient between the weekly OMI-AI and the AOT_{440} reaches 0.70 compared to 0.62 at a daily time-step and in Banizoumbou, it reaches 0.78 compared to 0.68 at a daily time-step. The slopes of the linear regression show the same East–West gradient with consistent values compared to the daily time-step at both sites. Regarding the correlation coefficients between the weekly OMI-AI and the PM_{10}, they reach 0.49 in Cinzana (compared to 0.36 at a daily time-step), and 0.45 in Banizoumbou (compared to 0.37 at a daily time-step). As a conclusion, the temporal integration of the aerosol parameters over one week significantly increases the agreement between the remotely sensed aerosol index and the ground-based measurements. More specifically, the OMI-AI is more representative of the aerosol concentrations at the surface at the weekly scale than at the daily scale. This may be explained by the reduction of the PM_{10} concentration range (i.e., std PM_{10}) when increasing the averaging period (Fig. 3). Furthermore, the weekly time-step is in agreement with the typical duration of the dust storms which range from 1 to 6 days with mean of 2.5 days (Marticorena et al., 2010).

The final step of the comparison is to examine the capability of the OMI-AI to reproduce the annual cycle of the mineral dust content derived from the AOT_{440} and PM_{10}. It is particularly important to evaluate whether the weekly OMI-AI data set provides a consistent calendar compared to ground-based aerosol measurements. Indeed the influence of dust on meningitis is suspected to occur mainly during the increasing phase of the epidemics in the first trimester of the year. The weekly standardized mean annual cycles presented in Fig. 6 are computed from the values of Fig. 5 by subtracting the mean from each weekly value, then dividing by the standard deviation. For each variable, a clear annual cycle is observed at both Cinzana and Banizoumbou, mainly positive at the beginning of the year and crossing zero in July. From August to December the three parameters stay in agreement whereas three periods could be distinguished from January to July: from January to March, the core of the dry season; from April to May, the transition to the wet season; from June to July, the wet season settlement. During the first trimester, the aerosol layer is located close to the surface and a PM_{10} maximum is obtained before week 10 (early March), which is consistent with dust-laden winds coming from the North-East (Harmattan winds) at this period. From April to early May, the AOT_{440} maximum happens generally between week 13 to week 18. Finally, from late May to June the OMI-AI maximum occurs around week 25 when the PM_{10} concentrations are already low. Consequently, the dust transport moves in higher altitudes and seems to be disconnected from the surface. All these behaviors are shared by the two stations in average for the period 2006–2008. Counter intuitively for the OMI-AI and PM_{10} relationship, the correlation coefficient during the core of the dry season (0.35 in Cinzana and 0.41 in Banizoumbou) is lower than during the wet season (0.64 in Cinzana and 0.62 in Banizoumbou). This means that the linear assumption is not verified during the first trimester, which may be due to the high dust variability at this period of the year, better captured by the PM_{10} surface measurements. Moreover, the slope of the OMI-AI and PM_{10} relationship is expected to change along the year. Nevertheless, the weekly time-step improves the correlations between the OMI-AI and the PM_{10} concentration (Table 5 compared to Fig. 5). On average, during the core of the dry season, the OMI-AI and PM_{10} both experience an increasing phase. This agreement is not retrieved for the other periods of the year, and especially from April to June (Fig. 6): the OMI-AI tends to increase when the PM_{10} decreases.

Fig. 7 presents the OMI-AI, AOT_{440}, and PM_{10} time-series for the individual years 2006, 2007 and 2008. When looking at the PM_{10} ("the ground truth") for each year considered, the same events are retrieved by both stations during the first trimester. Banizoumbou monitored usually stronger dust episodes than Cinzana, which is consistent with the distance to the sources and the wind direction (Nord-East). This difference seems less clear for the AOT_{440} even though the AOT_{440} time-series are phased with those of PM_{10}. The OMI-AI identifies the dust events both in Cinzana and Banizoumbou during the core of the dry season and this is associated with moderate values ($\approx$2). The other important result for the OMI-AI is that it systematically experiences high values from April to June (from 2 to 3), and it decreases from July to September (from 2 to 1). Both in Banizoumbou and in Cinzana, an intense dust peak is recorded on the 8th of March 2006 (Fig. 7a and b) due to a continental dust storm (Slingo et al., 2006). This outstanding event leads to the yearly maximum for the sun photometers (AOT_{440}) and TEOM measurement (PM_{10}), which also appears in the cycles of the Fig. 6a and b. For the OMI-AI however, this event leads to a local maximum in the first trimester but with only a moderate value considering the entire year. To conclude, focusing on the onset–peak period of the meningitis epidemics (January–March), the weekly dynamics of the OMI-AI, AOT_{440} and PM_{10} are consistent, whereas during the second trimester of the year (April–June), the OMI-AI increases, losing gradually the surface representativity.

Table 5
Correlation coefficient between OMI-AI and PM_{10} concentration temporally averaged at ±1 h around the satellite overpass time (column "overpass"), at ±5 h around the satellite overpass time (column "day"), at ±12 h around the satellite overpass time (column "24 h") for the whole year.

	Overpass		Day		24 h	
	R	*N*	*R*	*N*	*R*	*N*
Cinzana	0.34	942	0.36	961	0.36	961
Banizoumbou	0.40	890	0.37	896	0.27	896
All sites	0.36	1832	0.35	1857	0.27	1857

3.3. A case study: OMI-AI and meningitis epidemics

The Harmattan winds have been proved to play on the timing of the meningitis epidemics (Sultan et al., 2005) and, to a lesser extent, their intensities (Yaka et al., 2008). Recently, the desert dust has been

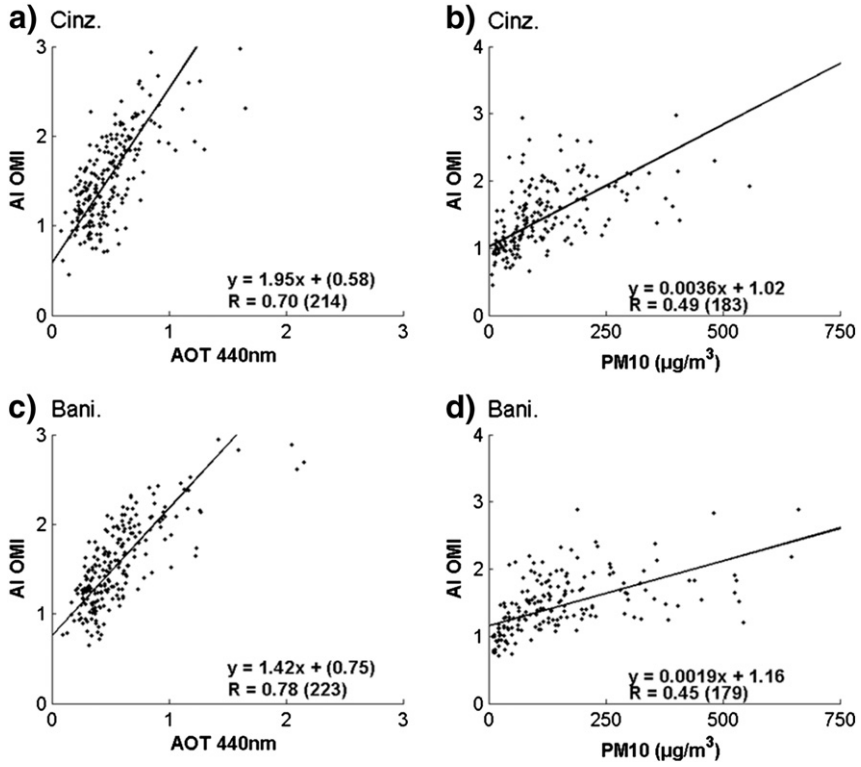

Fig. 5. (Left) scatter plot between weekly OMI-AI and AOT_{440} for the period 2006–2008 (whole year) in: a) Cinzana (Mali); c) Banizoumbou (Niger). (Right) scatter plot between weekly OMI-AI and PM_{10} concentrations for the period 2006–2009 in: b) Cinzana (Mali); d) Banizoumbou (Niger).

shown to impact on the meningitis incidence in West Africa (Martiny & Chiapello, in press). The onset of the meningitis season has been shown to be tightly related to dust flowing close to the surface from February to April because each meningitis peak has been shown to be preceded by a dust peak with a lead-time (ranging from 0 to 2 weeks). The most common explanation is that extreme air dryness combined with high dust loads that persists until the end of the dry season can damage the pharyngeal mucosa. As a result, the colonizing meningococci are more likely to invade the epithelium (Mueller & Gessner, 2010). High dust loads persisting over weeks or extreme dust events may thus favor the meningococcal to pass into the blood. According to this hypothesis dust could be considered as a trigger of the epidemics. However, other mechanisms are

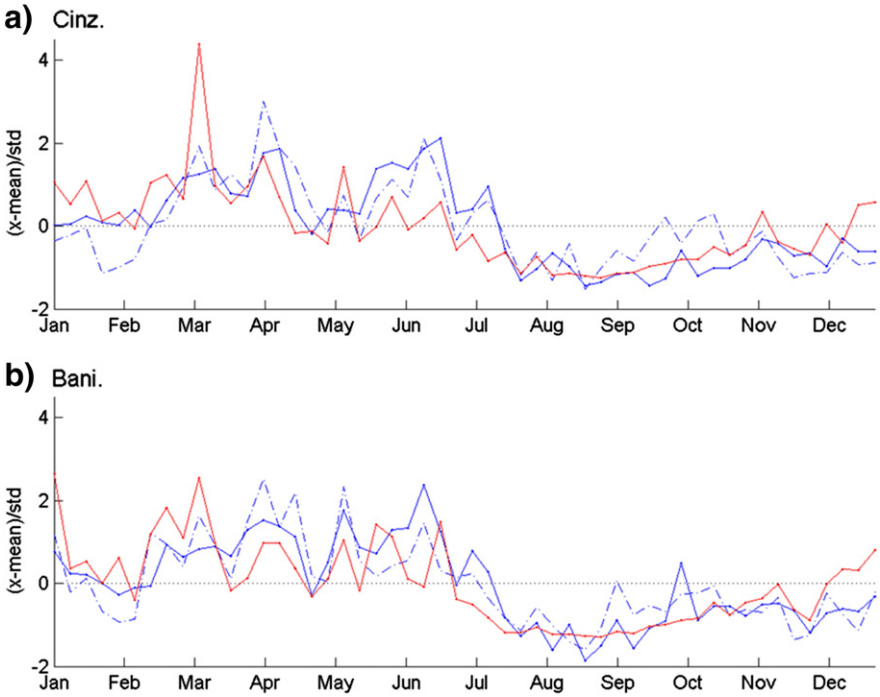

Fig. 6. Comparison between OMI-AI (blue), AOT_{440} (dashed blue) and PM_{10} concentration (red) standardized mean annual cycles for the period 2006–2008 at a weekly time-step in a) Cinzana (Mali). b) Banizoumbou (Niger) (For interpretation of the references to color in this figure, the reader is referred to the web version of this article.).

also possible which impact the bacteria carriage ratio by affecting the airborne dryness (thus the transmission likelihood), by preceding viral infection, by increasing the cough or people grouping during the night (e.g., Greenwood et al., 1984; Thomson et al., 2006, 2009; Mueller & Gessner, 2010). Another hypothesis is that mineral dust may bring iron into the bacteria, a nutrient required for bacteria growth (Jordan & Saunders, 2009) but there is only a little proportion of soluble iron in mineral dust (Zhu et al., 1997). Due to the difficulty in separating all these effects, dust load could be seen as a proxy of the intensity of all those mechanisms.

Until now, we have demonstrated the ability of the OMI-AI to represent the weekly ground dust concentration during the dry season. Assuming dust plays a role of trigger of the epidemics, a delay is expected between the dust concentration and the meningitis incidence increases. This time-lag should range from one to several weeks, due to the incubation time of the bacteria (Stephens et al., 2007). To test this hypothesis, the mean annual cycles of the national incidence (NI) is compared with the one of the OMI-AI in Burkina Faso, Mali or Niger. OMI-AI values have been extracted and averaged at a national scale. The NI has been correlated with the national AI with several time-lags from 0 to 4 weeks over two periods: (C1) trimester 1 (January–March) roughly corresponding to onset–maximum peak dates; (C2) trimesters 1 and 2 (January–June) roughly corresponding to the whole meningitis season. Our previous results have suggested that during the trimester 1, the OMI-AI is better linked to dust conditions at the surface, whereas the vertical distribution makes the OMI-AI more influenced by higher altitude aerosol layers during the trimester 2.

The important result shown by this analysis is that the determination coefficient (R^2) reaches high values in the three countries for a constant time-lag between the NI and the OMI-AI (Table 6). When considering the C1 period, R^2 is high for time-lags ranging from 0 to 2 weeks and maximum for a 1-week time-lag in the three countries ($R^2 = 0.73$ in Burkina Faso, $R^2 = 0.80$ in Niger and $R^2 = 0.89$ in Mali). The loss of consistence is clear for the period C2 (i.e., R^2 is null). The sensitivity to the number of weeks used to estimate the correlation for C1 and C2 is very low (i.e., ± 2 weeks), reinforcing our conclusion. There is a clear decrease of the correlation between C1 and C2 which occurs around week 18 (i.e., early May). This suggests that April could be included in the C1 period. However, our previous results suggest that April must be carefully considered because this is the period of the highest AOT_{440}.

The increase of mineral aerosols as represented by the OMI-AI seems to match with the increasing phase of the epidemic season (C1). This preliminary analysis is consistent with the existence of a link between the OMI-AI and NI until March with a 1-week time-lag at the scale of the country. This encourages further investigations at a finer spatial scale such as the district scale. The 1-week time-lag suggests synchronization because dust floating close to the surface (period C1) may play a role in the increase of the meningitis cases, likely in association with specific meteorological conditions. For instance, Martiny and Chiapello (in press) illustrated the particular role of dust during the dry season on the onset and the intra-seasonal variability of the meningitis season. As a next step, the AI as well as other atmospheric parameters (such as humidity, temperature and wind) need to be taken into account to continue previous analyses made at the national scale (Martiny & Chiapello, in press; Sultan et al., 2005; Yaka et al., 2008) in order to better understand and forecast dust impacts on the onset, maximum and ending of the epidemics.

4. Discussion and conclusions

This study is dedicated to the evaluation of the suitability of the aerosol index (AI) from the ozone monitoring instrument (OMI) for dust impact studies on health in West Africa. Satellite data sets are powerful observation tools that can help to better understand the complex relationships between climate, dust and diseases, as they are available every day at a global scale. Over four years of OMI-AI data along with ground-based AERONET sun photometer AOT_{440}, and TEOM PM_{10} have been analyzed over the Sahel. The main question addressed by

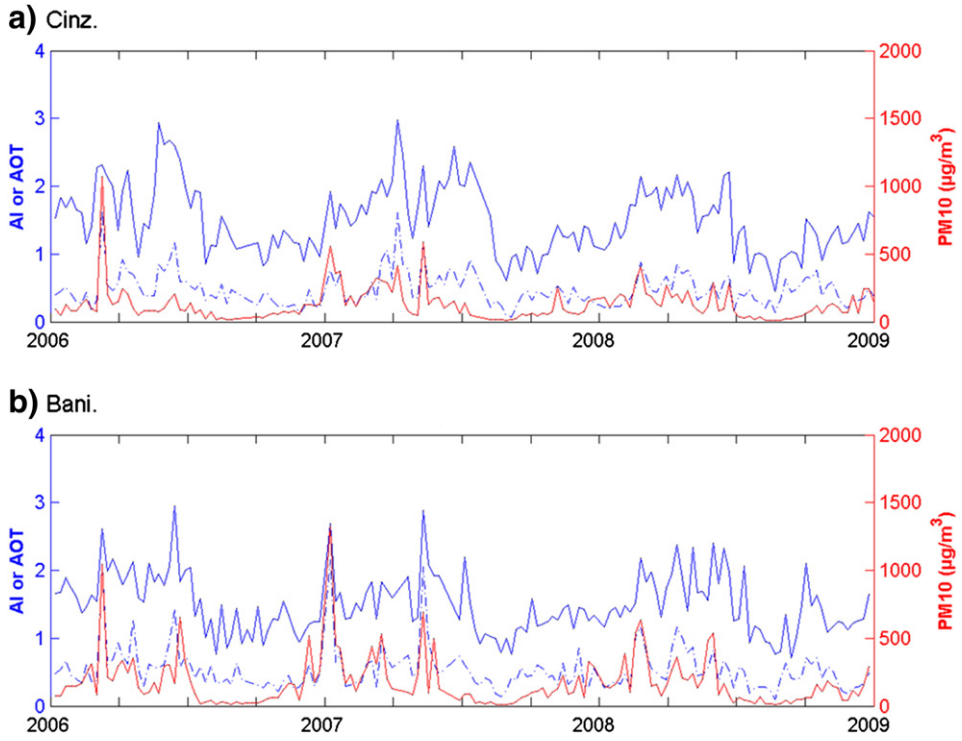

Fig. 7. Comparison between OMI-AI (blue), AOT_{440} (dashed blue) and PM_{10} concentration (red) for the period 2006–2008 at a weekly time-step in a) Cinzana (Mali). b) Banizoumbou (Niger) (For interpretation of the references to color in this figure, the reader is referred to the web version of this article.).

Table 6
Analysis of the OMI-AI/NI relationships: determination coefficients R^2 between the OMI-AI and national incidence (NI) considering different time-lags (from 0 to 4 weeks) and two distinct periods (trimester 1: "C1 column"; trimesters 1 and 2: "C2 column").

	Burkina Faso		Niger		Mali	
	C1	C2	C1	C2	C1	C2
Lag 0	0.61	0.14	0.74	0.01	0.82	0.00
Lag 1	0.73	0.15	0.80	0.00	0.89	0.00
Lag 2	0.68	0.12	0.77	0.01	0.87	0.00
Lag 3	0.55	0.07	0.70	0.02	0.71	0.00
Lag 4	0.43	0.03	0.68	0.03	0.56	0.01

this analysis is: How to use the OMI-AI to investigate mineral dust impacts on health, and specifically meningitis epidemics, in the Sahel?

First of all, the OMI-AI is consistent with the AOT_{440} measurements acquired on four Sahelian sites, for the whole year as well as for the core of the dry season (i.e., January–March), at the time of the satellite overpass, at the daily or at the weekly time-step. This means that the OMI-AI is significantly related to the AOT_{440}, which represents the vertically integrated dust load. Secondly, the ground-based AOT_{440} has been shown to be related to the PM_{10} at the time of the OMI overpass, at the daily or at the weekly time-step. The correlations between the OMI-AI and PM_{10} in Niger (Banizoumbou) and Mali (Cinzana) explain less than 30% of the variance at a daily time-step. An important benefit for the variance is observed for the correlation between the OMI-AI and the PM_{10} concentrations from the daily to the 3-day average (i.e., up to 30%) and slightly increase from the 3-day to the weekly average, in agreement with an average dust event duration of 2.5 days (Marticorena et al., 2010).

Focusing now on the OMI-AI, AOT_{440} and PM_{10} annual cycle comparison, for the two PM_{10} stations, the maximum date happens in late March for the PM_{10}, in April–early May for the AOT_{440} and in June for the OMI-AI. During the core of the dry season, at both locations the PM_{10} maximum happens during the same week every year due to strong Harmattan winds. The transition to the wet season starts in April when the temperature is the highest and the surface pressure is the lowest associated with convection (Lavaysse et al., 2009). It coincides with the highest AOT_{440} and high OMI-AI values, thus a maximum of the vertically integrated dust transported over the Sahel. The ratio of AOT_{440} divided by PM_{10} increases, suggesting a change in the aerosol vertical distribution compared to the core of the dry season. Then in May, the pre-onset of the monsoon happens when the inter-tropical front (the discontinuity in the wind direction) moves northward reaching the Sahel (Sultan et al., 2003). This front pushes in altitude the Harmattan flux and creates the Saharan Air Layer, leading to dust events in altitude captured by the OMI-AI time-series and not by the PM_{10} measurements. Therefore, from April to June, the OMI-AI surface representativity decreases gradually until the monsoon flux arrival from the South. When the monsoon is clearly established, the OMI-AI remains high until July, whereas PM_{10} concentrations are already low. Thus, there is a temporal shift between the maxima of the annual cycles in OMI-AI, AOT_{440} and PM_{10}. However, during the first trimester of the year, the strong dust events recorded in the PM_{10} measurements, lead to local maxima in the time-series of the OMI-AI at Banizoumbou and Cinzana (Fig. 7). This means that the OMI-AI in the core of the dry season (the increase phase of the meningitis season) is able to reproduce the weekly variability of the AOT_{440} and the PM_{10} measurements and to detect the dust events when the dust concentrations at the surface are the highest. This is a very important result in terms of dust impact studies on health. An effect of the high dust concentration is expected after several weeks (e.g., De Longueville et al., 2010; Mueller & Gessner, 2010). Martiny and Chiapello (in press) suggest that dust may play a role on the onset of the meningitis season and its variability, especially from January to March. During this period, our results show that it is possible to use OMI-AI to investigate the links between dust and meningitis. Indeed, for this period, the OMI-AI can be considered as representative of the weekly surface dust concentrations. This is satisfactory given the weekly time-step of the available epidemiological data sets. Even though the variance of PM_{10} explained by the OMI-AI is lower than 50%, the timing of the dust concentration increase is well captured by the OMI-AI. For the period January–March, (i.e., from the onset to the maximum peak date), the correlation between the OMI-AI and the meningitis incidence at the national scale suggests a one week delay between the increase of dust load and of the epidemics. This delay may signify that dust acts as a trigger of the epidemics. The elaboration of a dust persistence index based on the OMI-AI at the district scale should be possible. Such an index could be used to investigate the effect of dust integrated over the whole dry season. The numerical model of the emission/transport/deposition of dust such as CHIMERE (Menut et al., 2009; Schmechtig et al., 2011), could also be tested for specific skills needed, as it has been done for ozone and mortality (Valari et al., 2011). The OMI-AI could also be included in meningitis early warning systems, such as those currently operational in Burkina Faso and Niger based on climate variables only, which explain 25% of the variance in meningitis (Yaka et al., 2008).

Finally, our study has been achieved using the PM_{10} and AOT_{440} measurements acquired at two Sahelian sites more than 1000 km apart. A difference in the slope of the OMI-AI/AOT_{440} (or OMI-AI/PM_{10}) relationships is observed from West to East which can be explained by a lower altitude of the dust layer near the sources (Engelstaedter & Washington, 2007b). The differences noticed in the weekly PM_{10} time-series between Banizoumbou and Cinzana are also observed by the OMI-AI during the core of the dry season. Our analysis is based on a spatially averaged OMI-AI (3×3 pixels) around the stations, showing the ability of the OMI-AI to provide relevant information on the dust surface concentration at a 0.75° resolution. The dust events are recorded at the two stations, suggesting a regional to continental scale of the dust events with several days of duration (Marticorena et al., 2010). Thus, spatial patterns of dust at the weekly time-step may concern a larger area than 0.75° with weak local differences inside. This suggests that the coarser resolution of the TOMS-AI would not prevent its use to detect dust episodes and monitor the weekly variability during the core of the dry season in the Sahel. The advantage of the TOMS-AI time series is to cover two important epidemics in 1986 and in 1996/1997 as a decadal cycle of the meningitis epidemics has been shown in West Africa (Broutin et al., 2007). Preliminary comparisons between TOMS-AI and AOT_{440} provided similar correlation coefficients than with the OMI-AI. A combination of homogenized TOMS-AI and OMI-AI time-series would allow the investigation of the link between dust and meningitis epidemics over decades (TOMS: 1978–1993 and 1996–2005; OMI: 2004–2009).

To conclude, this study highlights the fact that the satellite aerosol products can improve our knowledge of the complex relationships between dust and diseases during the relevant period of high dust load, in regions such as the Sahel where stations measuring dust surface concentrations are rare.

Acknowledgments

This work was achieved in the framework of the ADCEM project (impacts of Desert Aerosols and Climate on Meningitis Epidemics in the Sahel) of the Paris Climate-Environment-Society consortium (http://www.gisclimat.fr/en) and funded by the ANSES (Agence Nationale de SEcurité Sanitaire de l'alimentation, de l'environnement et du travail). The study was also supported by the French component of the African Monsoon Multidisciplinary Analysis (AMMA) International program. Based on a French initiative, AMMA was built by an international scientific group and is currently funded by a large number of agencies, especially from France, UK, US and Africa. It has been the beneficiary of a major financial contribution from the European Community's Sixth Framework Research Program. The authors are grateful to the WHO for providing meningitis epidemiological data, and the LOA for providing

the AOT data for the AERONET/PHOTONS stations. We thank the PI investigators and their staff for establishing and maintaining the four sites used in this study. Calculations were performed using HPC resources from DSI-CCUB (Université de Bourgogne).

References

Agier, L., Broutin, H., Bertherat, E., Djingarey, M. H., Lingani, C., Perea, W., et al. (2013). *Timely detection of bacterial meningitis epidemics at district level: A study in three countries of the African meningitis belt* (pp. 30–36). Oxford University Press.

Ayers, G. P. (2001). Comment on regression analysis of air quality data. *Atmospheric Environment*, *35*, 2423–2425.

Broutin, H., Philippon, S., de Magny, G. C., Courel, M. F., Sultan, B., & Guegan, J. F. (2007). Comparative study of meningitis dynamics across nine African countries: A global perspective. *International Journal of Health Geographics*, *6–29*, http://dx.doi.org/10.1186/1476-072X-6-29.

Campagne, G., Schuchat, A., Djibo, S., Ousseini, A., Cisse, L., & Chippaux, J. P. (1999). *Epidemiology of bacterial meningitis in Niamey, Niger, 1981–96* (pp. 499–508) World Health Organization.

Carboni, E., Thomas, G. E., Sayer, A. M., Siddans, R., Poulsen, C. A., Grainger, R. G., et al. (2012). Intercomparison of desert dust optical depth from satellite measurements. *Atmospheric Measurement Techniques*, *5*, 1973–2002.

Cavalieri, O., Cairo, F., Fierli, F., Di Donfrancesco, G., Snels, M., Viterbini, M., et al. (2010). Variability of aerosol vertical distribution in the Sahel. *Atmospheric Chemistry and Physics*, *10*, 12005–12023.

Chiapello, I., & Moulin, C. (2002). TOMS and Meteosat satellite records of the variability of Saharan dust transport over the Atlantic during the last two decades (1979–1997). *Geophysical Research Letters*, *29*, 17-11–17-14.

Chiapello, I., Moulin, C., & Prospero, J. M. (2005). Understanding the long-term variability of African dust transport across the Atlantic as recorded in both Barbados surface concentrations and large-scale total ozone mapping spectrometer (TOMS) optical thickness. *Journal of Geophysical Research*, *110*, D18S10.

Chiapello, I., Prospero, J. M., Herman, J. R., & Hsu, N. C. (1999). Detection of mineral dust over the North Atlantic Ocean and Africa with the Nimbus 7 TOMS. *Journal of Geophysical Research*, *104*, 9277–9291.

Christopher, S. A., Gupta, P., Haywood, J., & Greed, G. (2008). Aerosol optical thicknesses over North Africa: 1. Development of a product for model validation using ozone monitoring instrument, multiangle imaging spectroradiometer, and aerosol robotic network. *Journal of Geophysical Research*, *113*, D00C04.

Cohen, W. B., Maiersperger, T. K., Gower, S. T., & Turner, D. P. (2003). An improved strategy for regression of biophysical variables and Landsat ETM+ data. *Remote Sensing of Environment*, *84*, 561–571.

De Graaf, M., Stammes, P., Torres, O., & Koelemeijer, R. B. A. (2005). *Absorbing aerosol index: Sensitivity analysis, application to GOME and comparison with TOMS*. Washington, DC: ETATS-UNIS: American Geophysical Union.

De Longueville, F., Henry, S., & Ozer, P. (2009). Saharan dust pollution: Implications for the Sahel? *Epidemiology*, http://dx.doi.org/10.1097/EDE.0b013e3181afef49.

De Longueville, F., Hountondji, Y. -C., Henry, S., & Ozer, P. (2010). What do we know about effects of desert dust on air quality and human health in West Africa compared to other regions? *The Science of the Total Environment*, *409*, 1–8.

Eck, T. F., Bhartia, P. K., Hwang, P. H., & Stowe, L. L. (1987). Reflectivity of earth's surface and clouds in ultraviolet from satellite observations. *Journal of Geophysical Research*, *92*, 4287–4296.

Engelstaedter, S., Tegen, I., & Washington, R. (2006). North African dust emissions and transport. *Earth-Science Reviews*, *79*, 73–100.

Engelstaedter, S., & Washington, R. (2007a). Atmospheric controls on the annual cycle of North African dust. *Journal of Geophysical Research*, *112*, D03103.

Engelstaedter, S., & Washington, R. (2007b). Temporal controls on global dust emissions: The role of surface gustiness. *Geophysical Research Letters*, *34*, L15805.

Ginoux, P., & Torres, O. (2003). Empirical TOMS index for dust aerosol: Applications to model validation and source characterization. *Journal of Geophysical Research*, *108*, 4534.

Goudie, A. S., & Middleton, N. J. (2001). Saharan dust storms: Nature and consequences. *Earth-Science Reviews*, *56*, 179–204.

Greenwood, B. (1999). Meningococcal meningitis in Africa. *Transactions of the Royal Society of Tropical Medicine and Hygiene*, *93*, 341–353.

Greenwood, B. M., Bradley, A. K., Blakebrough, I. S., Wali, S., & Whittle, H. C. (1984). Meningococcal disease and season in sub-Saharan Africa. *The Lancet*, *323*, 1339–1342.

Gyan, K., Henry, W., Lacaille, S., Laloo, A., Lamsee-Ebanks, C., McKay, S., et al. (2005). African dust clouds are associated with increased paediatric asthma accident and emergency admissions on the Caribbean island of Trinidad. *International Journal of Biometeorology*, *49*, 371–376.

Haywood, J. M., Pelon, J., Formenti, P., Bharmal, N., Brooks, M., Capes, G., et al. (2008). Overview of the dust and biomass-burning experiment and African Monsoon Multidisciplinary Analysis special observing period-0. *Journal of Geophysical Research-Atmospheres*, *113*, 20.

Herman, J. R., Bhartia, P. K., Torres, O., Hsu, C., Seftor, C., & Celarier, E. (1997). Global distribution of UV-absorbing aerosols from Nimbus 7/TOMS data. *Journal of Geophysical Research*, *102*, 16911–16922.

Herman, J. R., & Celarier, E. A. (1997). Earth surface reflectivity climatology at 340–380 nm from TOMS data. *Journal of Geophysical Research-Atmospheres*, *102*, 28003–28011.

Holben, B. N., Eck, T. F., Slutsker, I., Tanre, D., Buis, J. P., Setzer, A., et al. (1998). AERONET — A federated instrument network and data archive for aerosol characterization. *Remote Sensing of Environment*, *66*, 1–16.

Holben, B. N., Tanre, D., Smirnov, A., Eck, T. F., Slutsker, I., Abuhassan, N., et al. (2001). An emerging ground-based aerosol climatology: Aerosol optical depth from AERONET. *Journal of Geophysical Research-Atmospheres*, *106*, 12067–12097.

Hsu, N. C., Herman, J. R., Torres, O., Holben, B. N., Tanre, D., Eck, T. F., et al. (1999). Comparisons of the TOMS aerosol index with sun-photometer aerosol optical thickness: Results and applications. *Journal of Geophysical Research-Atmospheres*, *104*, 6269–6279.

Hsu, N. C., Tsay, S. C., King, M. D., & Herman, J. R. (2004). Aerosol properties over bright-reflecting source regions. *IEEE Transactions on Geoscience and Remote Sensing*, *42*, 557–569.

Jordan, P. W., & Saunders, N. J. (2009). Host iron binding proteins acting as niche indicators for *Neisseria meningitidis*. *PLoS One*, *4*, 13.

Lapeyssonnie, L. (1963). Cerebrospinal meningitis in Africa. *Bulletin of the World Health Organization*, *28*, 1–114 (Suppl.).

Laurent, B., Marticorena, B., Bergametti, G., Leon, J. F., & Mahowald, N. M. (2008). Modeling mineral dust emissions from the Sahara desert using new surface properties and soil database. *Journal of Geophysical Research-Atmospheres*, *113*, 20, http://dx.doi.org/10.1029/2007JD009484.

Lavaysse, C., Flamant, C., Janicot, S., Parker, D., Lafore, J. P., Sultan, B., et al. (2009). Seasonal evolution of the West African heat low: A climatological perspective. *Climate Dynamics*, *33*, 313–330.

Legrand, M., Bertrand, J. J., Desbois, M., Menenger, L., & Fouquart, Y. (1989). The potential of infrared satellite data for the retrieval of Saharan-dust optical depth over Africa. *Journal of Applied Meteorology*, *28*, 309–319.

Legrand, M., Plana-Fattori, A., & N'Doumé, C. (2001). Satellite detection of dust using the IR imagery of Meteosat 1. Infrared difference dust index. *Journal of Geophysical Research*, *106*, 18251–18274.

Léon, J. F., Derimian, Y., Chiapello, I., Tanré, D., Podvin, T., Chatenet, B., et al. (2009). Aerosol vertical distribution and optical properties over M'Bour (16.96° W; 14.39° N), Senegal from 2006 to 2008. *Atmospheric Chemistry and Physics*, *9*, 9249–9261.

Levelt, P. F., van den Oord, G. H. J., Dobber, M. R., Malkki, A., Huib, V., Johan de, V., et al. (2006). The ozone monitoring instrument. *IEEE Transactions on Geoscience and Remote Sensing*, *44*, 1093–1101.

Mahowald, N. M., & Dufresne, J. -L. (2004). Sensitivity of TOMS aerosol index to boundary layer height: Implications for detection of mineral aerosol sources. *Geophysical Research Letters*, *31*, L03103.

Mann, M. E., Bradley, R. S., & Hughes, M. K. (1998). Global-scale temperature patterns and climate forcing over the past six centuries. *Nature*, *392*, 779–787.

Marticorena, B., Chatenet, B., Rajot, J. L., Traore, S., Coulibaly, M., Diallo, A., et al. (2010). Temporal variability of mineral dust concentrations over West Africa: Analyses of a pluriannual monitoring from the AMMA Sahelian dust transect. *Atmospheric Chemistry and Physics*, *10*, 8899–8915.

Martiny, N., & Chiapello, I. (in press). *Assessments for the impact of mineral dust on the meningitis incidence in West Africa. Atmospheric Environment*, http://dx.doi.org/10.1016/j.atmosenv.2013.01.016.

Martonchik, J. V., Diner, D. J., Kahn, R., Gaitley, B., & Holben, B. N. (2004). Comparison of MISR and AERONET aerosol optical depths over desert sites. *Geophysical Research Letters*, *31*, L16102.

Menut, L., Chiapello, I., & Moulin, C. (2009). Predictability of mineral dust concentrations: The African Monsoon Multidisciplinary Analysis first short observation period forecasted with CHIMERE-DUST. *Journal of Geophysical Research*, *114*, D07202.

Molesworth, A. M., Cuevas, L. E., Connor, S. J., Morse, A. P., & Thomson, M. C. (2003). Environmental risk and meningitis epidemics in Africa. *Emerging Infectious Diseases*, *9*, 1287–1293.

Molesworth, A. M., Thomson, M. C., Connor, S. J., Cresswell, M. P., Morse, A. P., Shears, P., et al. (2002). Where is the meningitis belt? Defining an area at risk of epidemic meningitis in Africa. *Transactions of the Royal Society of Tropical Medicine and Hygiene*, *96*, 242–249.

Morales, C. (1986). The airborne transport of Saharan dust: A review. *Climatic Change*, *9*, 219–241.

Mueller, J. E., & Gessner, B. D. (2010). A hypothetical explanatory model for meningococcal meningitis in the African meningitis belt. *International Journal of Infectious Diseases*, *14*, E553–E559.

N'Tchayi, G. M., Bertrand, J., Legrand, M., & Baudet, J. (1994). Temporal and spatial variations of the atmospheric dust loading throughout West Africa over the last thirty years. *Annales Geophysicae*, *12*, 265–273.

Ogunjobi, K. O., He, Z., & Simmer, C. (2008). Spectral aerosol optical properties from AERONET sun-photometric measurements over West Africa. *Atmospheric Research*, *88*, 89–107.

Pelletier, B., Santer, R., & Vidot, J. (2007). Retrieving of particulate matter from optical measurements: A semiparametric approach. *Journal of Geophysical Research*, *112*, D06208.

Péré, J. C., Pont, V., Mallet, M., & Bessagnet, B. (2009). Mapping of PM10 surface concentrations derived from satellite observations of aerosol optical thickness over South-Eastern France. *Atmospheric Research*, *91*, 1–8.

Perez, L., Tobias, A., Querol, X., Künzli, N., Pey, J., Alastuey, A., et al. (2008). Coarse particles from Saharan dust and daily mortality. *Epidemiology (Cambridge, Mass.)*, *19*, 800–807.

Pinker, R. T., Pandithurai, G., Holben, B. N., Dubovik, O., & Aro, T. O. (2001). A dust outbreak episode in sub-Sahel West Africa. *Journal of Geophysical Research*, *106*, 22923–22930.

Prospero, J. M., Blades, E., Naidu, R., Mathison, G., Thani, H., & Lavoie, M. C. (2008). Relationship between African dust carried in the Atlantic trade winds and surges in pediatric asthma attendances in the Caribbean. *International Journal of Biometeorology*, *52*, 823–832.

Prospero, J. M., Ginoux, P., Torres, O., Nicholson, S. E., & Gill, T. E. (2002). Environmental characterization of global sources of atmospheric soil dust identified with the Nimbus 7 total ozone mapping spectrometer (TOMS) absorbing aerosol product. *Reviews of Geophysics*, *40*, 31.

Ramanathan, V., Crutzen, P. J., Kiehl, J. T., & Rosenfeld, D. (2001). Aerosols, climate, and the hydrological cycle. *Science*, *294*, 2119–2124.

Satheesh, S. K., Torres, O., Remer, L. A., Babu, S. S., Vinoj, V., Eck, T. F., et al. (2009). Improved assessment of aerosol absorption using OMI-MODIS joint retrieval. *Journal of Geophysical Research*, *114*, D05209.

Schmechtig, C., Marticorena, B., Chatenet, B., Bergametti, G., Rajot, J. L., & Coman, A. (2011). Simulation of the mineral dust content over Western Africa from the event to the annual scale with the CHIMERE-DUST model. *Atmospheric Chemistry and Physics*, *11*, 7185–7207.

Slingo, A., Ackerman, T. P., Allan, R. P., Kassianov, E. I., McFarlane, S. A., Robinson, G. J., et al. (2006). Observations of the impact of a major Saharan dust storm on the atmospheric radiation balance. *Geophysical Research Letters*, *33*, L24817.

Smirnov, A., Holben, B. N., Savoie, D., Prospero, J. M., Kaufman, Y. J., Tanre, D., et al. (2000). Relationship between column aerosol optical thickness and in situ ground based dust concentrations over Barbados. *Geophysical Research Letters*, *27*, 1643–1646.

Sokolik, I. N., Winker, D. M., Bergametti, G., Gillette, D. A., Carmichael, G., Kaufman, Y. J., et al. (2001). Introduction to special section: Outstanding problems in quantifying the radiative impacts of mineral dust. *Journal of Geophysical Research-Atmospheres*, *106*, 18015–18027.

Stephens, D. S., Greenwood, B., & Brandtzaeg, P. (2007). Epidemic meningitis, meningococcaemia, and *Neisseria meningitidis*. *The Lancet*, *369*, 2196–2210.

Sultan, B., Janicot, S., & Diedhiou, A. (2003). The West African monsoon dynamics. Part I: Documentation of intraseasonal variability. *Journal of Climate*, *16*, 3389–3406.

Sultan, B., Labadi, K., Guegan, J. F., & Janicot, S. (2005). Climate drives the meningitis epidemics onset in West Africa. *PLoS Medicine*, *2*, 43–49.

Thomson, M. C., Jeanne, I., & Djingarey, M. (2009). Dust and epidemic meningitis in the Sahel: A public health and operational research perspective. *IOP conference series: Earth and environmental science*, *7*. (pp. 012017).

Thomson, M. C., Molesworth, A. M., Djingarey, M. H., Yameogo, K. R., Belanger, F., & Cuevas, L. E. (2006). Potential of environmental models to predict meningitis epidemics in Africa. *Tropical Medicine & International Health*, *11*, 781–788.

Torres, O., Bhartia, P. K., Herman, J. R., Ahmad, Z., & Gleason, J. (1998). Derivation of aerosol properties from satellite measurements of backscattered ultraviolet radiation: Theoretical basis. *Journal of Geophysical Research*, *103*, 17099–17110.

Torres, O., Bhartia, P. K., Herman, J. R., Sinyuk, A., Ginoux, P., & Holben, B. (2002). A long-term record of aerosol optical depth from TOMS observations and comparison to AERONET measurements. *Journal of the Atmospheric Sciences*, *59*, 398–413.

Torres, O., Tanskanen, A., Veihelmann, B., Ahn, C., Braak, R., Bhartia, P. K., et al. (2007). Aerosols and surface UV products from ozone monitoring instrument observations: An overview. *Journal of Geophysical Research-Atmospheres*, *112*, 14.

Valari, M., Menut, L., & Chatignoux, E. (2011). Using a chemistry transport model to account for the spatial variability of exposure concentrations in epidemiologic air pollution studies. *Journal of the Air & Waste Management Association*, *61*, 164–179.

Washington, R., Todd, M. C., Lizcano, G., Tegen, I., Flamant, C., Koren, I., et al. (2006). Links between topography, wind, deflation, lakes and dust: The case of the Bodélé Depression, Chad. *Geophysical Research Letters*, *33*, L09401.

Washington, R., Todd, M., Middleton, N. J., & Goudie, A. S. (2003). Dust-storm source areas determined by the total ozone monitoring spectrometer and surface observations. *Annals of the Association of American Geographers*, *93*, 297–313.

Yahi, H., Santer, R., Weill, A., Crepon, M., & Thiria, S. (2011). Exploratory study for estimating atmospheric low level particle pollution based on vertical integrated optical measurements. *Atmospheric Environment*, *45*, 3891–3902.

Yaka, P., Sultan, B., Broutin, H., Janicot, S., Philippon, S., & Fourquet, N. (2008). Relationships between climate and year-to-year variability in meningitis outbreaks: A case study in Burkina Faso and Niger. *International Journal of Health Geographics*, *7*, 13.

Zender, C. S., & Kwon, E. Y. (2005). Regional contrasts in dust emission responses to climate. *Journal of Geophysical Research-Atmospheres*, *110*, 7.

Zhu, X. R., Prospero, J. M., & Millero, F. J. (1997). Diel variability of soluble Fe(II) and soluble total Fe in North African dust in the trade winds at Barbados. *Journal of Geophysical Research*, *102*, 21297–21305.